Electron Nuclear Double Resonance of a Series of Axially Liganded Protohemins and Deuterohemins

H. L. Van Camp,[1a] C. P. Scholes,*[1a] C. F. Mulks,[1a] and W. S. Caughey[1b]

Contribution from the Department of Physics, State University of New York at Albany, Albany, New York 12222, and the Department of Biochemistry, Colorado State University, Fort Collins, Colorado 80523. *Received April 15, 1977*

Abstract: ENDOR (electron nuclear double resonance) and EPR (electron paramagnetic resonance) signals were obtained from protohemin and deuterohemin dimethyl esters while axial anions were varied in the series: fluoride, formate, acetate, azide, chloride, and bromide. With the magnetic field along the fourfold symmetry axis of the hemin, we observed magnetic hyperfine interactions with the nitrogens and protons of the porphyrin and the halide ligands (F^-, Cl^-, and Br^-). The hemins were frozen in one of the following two solvent systems which hinder hemin aggregation and do not cause displacement of the axial anion: (I) a 1:1 (v/v) mixture of THF-$CHCl_3$; (II) a 1:1 (v/v) mixture of $CHCl_3$-CH_2Cl_2 that contained a fivefold molar excess, relative to hemin, of diamagnetic, metal-free mesoporphyrin. In a given solvent, differences of a few percent ($\leq$5%) in nitrogen hyperfine couplings were seen among different axial anions with no obvious correlation with other properties of the anion. The nitrogen couplings were significantly higher for all compounds in solvent II than in solvent I. In solvent II porphyrin meso proton hyperfine couplings increased ca. 6% as the axial ligand was changed from fluoride through bromide. This increase was consistent with meso proton chemical shifts seen previously by nuclear magnetic resonance (NMR) upon variation of axial anion. With solvent I ENDOR also showed that THF protons interact in a specific fashion with the hemin, with THF possibly acting as a sixth ligand. Previous hemoproton and nitrogen ENDOR results from metmyoglobin and methemoglobin are more closely mimicked by the results from solvent I than by those from solvent II.

ENDOR has previously been used to determine magnetic hyperfine and quadrupole interactions for hemin nitrogens, protons, iron, and chloride in both hemoproteins and hemin model systems.[2] In an initial study on protohemin chloride and protohemin bromide dimethyl esters,[2a] we observed by ENDOR a small change in nitrogen magnetic hyperfine couplings upon changing the axial anion from chloride to bromide. Hyperfine interactions were also seen with the halide nuclei themselves. Because hemins tend to aggregate and because spin-spin interactions between paramagnetic centers within an aggregate can totally eliminate ENDOR signals, we developed in ref 2a a solvent system to prevent hemin aggregation. This solvent system, referred to in this paper as solvent I, was a 1:1 (v/v) of solution of tetrahydrofuran (THF) and chloroform. It provided a glassy frozen matrix in which hemin esters would not aggregate, and as shown by the bromide and chloride hyperfine structure from hemins in it, the desired axial anion was not replaced by this solvent.

The purpose of our present study is to extend our ENDOR measurements to the detailed electronic effects of additional anions besides chloride and bromide: fluoride, acetate, formate, and azide. We deal in this paper with deuterohemins as well as protohemins. In the course of our present work we discovered proton ENDOR evidence that the THF of solvent I was interacting quite specifically with hemins. Therefore we developed an additional solvent system, referred to in this paper as solvent II, which also prevented aggregation of hemins, and differences in various hemin hyperfine parameters were noted between measurements in solvents I and II.

We expect that the results reported here will supplement already existing far-infrared (IR),[3a,b] Mössbauer,[3c,5b] proton nuclear magnetic resonance (NMR),[4] and near-IR[5] work on hemin compounds. In these previous studies systematic spectral changes were seen from hemins as one changed the axial anion in the series: fluoride, acetate, azide, chloride, bromide. The zero-field splittings from far-IR, the ^{57}Fe quadrupole splittings from Mössbauer, the hemoproton contact shifts from NMR, and the optical wavelengths from near-IR all increased in the series from fluoride through bromide. In ref 6 Caughey noted that the ligand order which these spectral properties followed was an order which corresponds to the inverse of the spectrochemical series. He noted that "these data may be generalized most simply in terms of stronger interaction or bonding between iron and axial ligand resulting in a weaker interaction between porphyrin nitrogens and iron".[6] We were motivated to do the present study because ENDOR is a good tool to determine directly and quantitatively from hyperfine and quadrupole couplings the way that electronic interactions and overlap with the heme nitrogen (and other atoms as well) may vary as we change the axial anion on heme.

Experimental Section

Apparatus. The ENDOR apparatus was previously described.[2a,7] The ENDOR cavity used here resonated near 9.2 GHz when loaded with sample, and it was even more lightly silvered than previous cavities so as to admit more ENDOR radiofrequency (rf) and to give rise to a higher percentage ENDOR signal. Chloride and nitrogen ENDOR signals were obtained with the absorption EPR mode (χ''), fairly large 100-kHz field modulation (~5 G peak to peak), fast ENDOR frequency sweeps (~10 MHz/s), and an ENDOR rf amplitude of ~1 G peak to peak. As we learned in ref 2e, proton ENDOR was best brought out by using the dispersion (χ') EPR mode, small field modulation (~0.5 G peak to peak), and slow ENDOR frequency sweeps (~0.1 MHz/s). The magnetic field and microwave frequencies were measured as described in ref 2a.

Reagents. All common solvents and salts were Fisher ACS Certified reagents. THF was distilled under an inert atmosphere over potassium immediately before use. $CHCl_3$ and CH_2Cl_2 were washed several times with distilled water, stored overnight over $CaCl_2$, and fractionally distilled immediately before use. The deuterated solvents THF-d_8, $CDCl_3$, and CD_2Cl_2 were purchased in 98% or better isotopic enrichment from Merck. NaCl with 90% enrichment in ^{37}Cl was purchased from Monsanto Chemical. Chloro iron(III) tetraphenylporphyrin (TPPFeCl) and octaethylporphyrin (OEPFeCl) were used to help in the assignment of hemin protons, and these were purchased from Strem Chemical Co. The TPPFeCl was recrystallized from CH_2Cl_2. Protohemin (hemin B) starting material was hemin equine type III from Sigma. Diamagnetic, metal-free mesoporphyrin dimethyl ester, purified by thin-layer chromatography, was purchased from Porphyrin Products, Logan, Utah. Deuterohemin esters were prepared at Fort Collins using methods previously reported.[8]

Protohemin IX Dimethyl Ester Iron(III) Derivatives. The preparation of protohemin esters described below was done at Albany. The initial stages of preparation of all protohemin esters through the stage of chromatography on alumina are described in ref 2a. The remainder of the preparation of chloride and bromide derivatives is described in ref 2a and the elemental analyses for these two compounds are listed

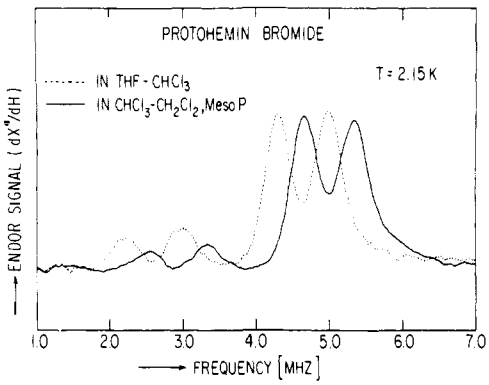

Figure 1. ENDOR spectrum from the nitrogens of protohemin bromide dimethyl ester in solvent I and in solvent II. The purpose of this figure is to show an increase in nitrogen hyperfine coupling upon going from solvent I to solvent II, and this increase is shown by the shift of the entire ENDOR pattern to higher frequency upon going from solvent I to solvent II. Both ENDOR spectra were taken at 5 G to the high-field side of the highest field peak in Figure 2. $T = 2.15$ K, $\nu_e \simeq 9.16$ GHz, $H \simeq 3.31$ kG, 100-kHz field modulation $\simeq 6$ G peak to peak, ENDOR rf $\simeq 1$ G peak to peak, and EPR done in the absorption mode. Microwave power was $\simeq 4$ μW for solvent I and $\simeq 0.3$ μW for solvent II.

below. Analyses were performed by A. Bernhardt, Mikroanalytisches Laboratorium, Elbach über Engelskirchen, West Germany. IR spectra of several of the samples in KBr were taken at Fort Collins.

Anal. Calcd for $C_{36}H_{36}ClFeN_4O_4$: C, 63.59; H, 5.34; N, 8.24; Cl, 5.21; Fe, 8.21. Found: C, 63.55; H, 5.34; N, 8.21; Cl, 4.99; Fe, 8.41.

Anal. Calcd for $C_{36}H_{36}BrFeN_4O_4$: C, 59.69; H, 5.01; N, 7.73; Br, 11.03; Fe, 7.70. Found: C, 59.96; H, 5.12; N, 7.78; Br, 10.79; Fe, 7.48.

In the preparation of protohemin IX dimethyl ester iron(III) *azide* the hemin ester eluent from the alumina chromatography was taken up in freshly distilled chloroform, shaken with a slightly acidified (with $HClO_4$) 1 M solution of NaN_3 to convert to the azide derivative, and passed through a column of dry sodium azide. The solution of protohemin ester was then crystallized from hot chloroform–isooctane, washed with isooctane, and dried at room temperature under vacuum.

Anal. Calcd for $C_{36}H_{36}FeN_7O_4$: C, 62.98; H, 5.29; N, 14.28; Fe, 8.13. Found: C, 62.73; H, 5.23; N, 14.16; Fe, 8.01.

In the preparation of protohemin IX dimethyl ester iron(III) *fluoride* the hemin ester eluent from the alumina chromatography was taken up in freshly distilled chloroform and shaken with a slightly acidified (with $HClO_4$) solution of 1 M KF. The chloroform was removed by flash evaporation, the protohemin was taken up in freshly distilled chloroform and filtered through glass wool, and the protohemin ester was precipitated with pentane. The precipitate was collected and dried under vacuum. ν_{FeF} in KBr was 581 cm^{-1}.

Anal. Calcd for $C_{36}H_{36}FFeN_4O_4$: C, 65.16; H, 5.47; N, 8.44; F, 2.86; Fe, 8.42. Found: C, 65.08; H, 5.47; N, 8.37; F, 2.79; Fe, 8.24.

In the preparation of protohemin IX dimethyl ester iron(III) *acetate* the hemin ester eluent of the alumina chromatography was taken up in glacial acetic acid and precipitated with pentane, and the precipitate was collected and dried under vacuum. The acetate ν_{CO} in KBr was 1659 cm^{-1}.

Anal. Calcd for $C_{38}H_{39}FeN_4O_6$: C, 64.87; H, 5.59; N, 7.96; Fe, 7.94. Found: C, 64.60; H, 5.63; N, 7.83; Fe, 8.04.

In the preparation of protohemin IX dimethyl ester iron(III) *formate* the hemin ester eluent of the alumina chromatography was taken up in freshly distilled chloroform, shaken with a slightly acidified (with HCOOH) 1 M solution of NaHCOO, and the chloroform layer dried by flash evaporation. The protohemin ester was taken up in freshly distilled chloroform, filtered through glass wool, precipitated with pentane, and dried under vacuum. Formate infrared bands occurred at 1655, 1386, and 1236–1217 cm^{-1} as measured in KBr.

Anal. Calcd for $C_{37}H_{37}FeN_4O_6$: C, 64.54; H, 5.42; N, 8.14; Fe, 8.11. Found: C, 64.18; H, 5.37; N, 7.99; Fe, 8.33.

Frozen Sample Preparation. Hemin sufficient for a 3 mM concentration was dissolved in one or the other of the solvent systems that we used and frozen immediately by plunging into liquid nitrogen. Sample volumes were about 1.5 mL. The systems were: solvent I, a 1:1 (v/v) mixture of THF and $CHCl_3$;[9] solvent II, a 1:1 mixture of CH_2Cl_2 and $CHCl_3$ that contained diamagnetic metal-free mesoporphyrin dimethyl ester in a fivefold molar ratio to paramagnetic hemin. The mesoporphyrin is needed in this system because in its absence the hemins will aggregate with each other. This system was patterned after a similar system, involving diamagnetic porphyrin, which was used to prevent aggregation of paramagnetic cupric porphyrins.[10]

Results

EPR Information. EPR spectra from hemins in both solvents I and II were typical high-spin spectra.[11] In the $g_e = 6$ region most EPR spectra indicated essentially an axial electronic symmetry, and the values of $g_e^{\perp}$, measured at the $d\chi''/dH$ zero crossing, were in the 5.8 to 5.9 range. Line widths between derivative extrema were in the 30 to 60 G range and hemins in solvent I typically had 10 to 20 G wider lines than their counterparts in solvent II. (Conceivably, the broader EPR line near $g_e = 6$ from hemins in solvent I could arise from small, solvent-induced rhombic perturbations to the hemin.) In solvent II fluorohemins gave well-resolved doublets in the $g_e = 6$ region with splittings of about 20 G, which we attribute to fluoride hyperfine structure.[12] A rhombic perturbation (E term in the spin Hamiltonian) has previously been seen from azidohemins by far-IR,[3b] and both proto- and deuterohemin azides in both solvents I and II gave evidence of rhombic splittings in the $g_e = 6$ region[13] with $E/D \simeq 0.02$.

In frozen solutions of high-spin hemins a peak in the $d\chi''/dH$ spectrum is characterisitcally found at the $g_e^{\parallel} = 2.00$ extremum. (See, for example, Figure 2 in ref 2c.) In fluoro- and bromohemins the EPR pattern near = 2.00 is respectively split into two or four peaks by interaction with the fluoride ($I = 1/2$) or bromide ($I = 3/2$) nucleus. Other hemins give only one peak at $g_e^{\parallel} = 2.00$.[14] The EPR signal at the $d\chi''/dH$ extremum will come from an oriented subset of hemes within the frozen solution which have the magnetic field normal to the porphyrin plane.[15] We perform ENDOR experiments while sitting on or above this $g_e^{\parallel}$ extremum. To obtain as well an oriented subset of heme molecules as possible (commensurate with decent ENDOR signal-to-noise) we often measure ENDOR at fields somewhat above the peak of the $g_e^{\parallel} = 2.00$ extremum or, in the case of the fluoro and bromo compounds, to the high-field side of the highest field peak of the fluoride or bromide hyperfine pattern.[16]

Nitrogen ENDOR. With the magnetic field along the porphyrin normal one obtains a four-line ENDOR pattern from the nitrogens, which indicates that for this orientation of the magnetic field the nitrogens are equivalent to each other. Such four-line ENDOR patterns are shown in Figure 1 for the nitrogens of protohemin bromide. We have fit the four ENDOR frequencies to eq 2 and obtain values of the magnetic hyperfine coupling, $|A_{zz}|$, and of the quadrupole coupling, $|P_{zz}|$.

In both solvents I and II magnetic hyperfine and quadrupole parameters were measured for all samples. We show in Table I these parameters as measured at the $d\chi''/dH$ extremum and 10 G to the high-field side of this extremum, which for the majority of samples was the highest field where one could still obtain adequate ENDOR signal-to-noise. If one keeps the solvent constant we note that the variation of nitrogen magnetic hyperfine and quadrupole couplings with axial anion is small. The chloride magnetic hyperfine couplings are higher than bromide in both solvents; fluoride magnetic hyperfine couplings are near the higher end of the series and the magnetic hyperfine couplings of the bromide near the lower end. The percentage change in the nitrogen parameters is not as large as the changes in the spectroscopic parameters measured by far-IR, Mössbauer, NMR, or near-IR. Depending on solvent, we note some rearrangements in the order with axial anion of magnetic hy-

Table I. ^{14}N ENDOR Results for Hemin Nitrogens

Compound	In THF-$CHCl_3$		In $CHCl_3$-Ch_2Cl_2 + mesoporphyrin	
	$\lvert A_{zz}\rvert$; $\lvert P_{zz}\rvert$, at $g_e^{\parallel}$ peak (in MHz)	$\lvert A_{zz}\rvert$; $\lvert P_{zz}\rvert$, at $g_e^{\parallel}$ peak + 10 G[a] (in MHz)	$\lvert A_{zz}\rvert$; $\lvert P_{zz}\rvert$, at $g_e^{\parallel}$ peak (in MHz)	$\lvert A_{zz}\rvert$; $\lvert P_{zz}\rvert$, at $g_e^{\parallel}$ peak + 10 G[a] (in MHz)
Proto-DME F^-	7.55 ± 0.02; 0.34 ± 0.01	7.54 ± 0.04; 0.36 ± 0.02	8.07 ± 0.03; 0.42 ± 0.02	7.99 ± 0.03; 0.41 ± 0.02
Proto-DME $HCOO^-$	7.37 ± 0.03; 0.38 ± 0.015	7.28 ± 0.06; 0.37 ± 0.03	7.69 ± 0.02; 0.42 ± 0.01	7.62 ± 0.03; 0.43 ± 0.02
Proto-DME AC^-	7.59 ± 0.04; 0.36 ± 0.02	7.48 ± 0.04; 0.37 ± 0.02	8.10 ± 0.02; 0.40 ± 0.01	8.03 ± 0.02; 0.40 ± 0.01
Proto-DME N_3^-	7.49 ± 0.02; 0.30 ± 0.01	7.45 ± 0.03; 0.31 ± 0.02	7.97 ± 0.04; 0.32 ± 0.02	7.98 ± 0.04; 0.32 ± 0.02
Proto-DME Cl^-	7.57 ± 0.03; 0.34 ± 0.02	7.41 ± 0.04; 0.37 ± 0.02	8.30 ± 0.025; 0.37 ± 0.02	8.10 ± 0.02; 0.35 ± 0.01
Proto-DME Br^-	7.37 ± 0.03; 0.34 ± 0.02	7.21 ± 0.07; 0.37 ± 0.04	8.03 ± 0.04; 0.36 ± 0.02	7.85 ± 0.04; 0.36 ± 0.02
Deutero-DME F^-	7.58 ± 0.02; 0.33 ± 0.01	7.54 ± 0.03; 0.36 ± 0.02	8.04 ± 0.02; 0.39 ± 0.01	8.03 ± 0.05; 0.41 ± 0.03
Deutero-DME N_3^-	7.46 ± 0.05; 0.29 ± 0.025	7.44 ± 0.06; 0.30 ± 0.03	7.85 ± 0.02; 0.33 ± 0.01	7.81 ± 0.02; 0.35 ± 0.01
Deutero-DME Cl^-	7.56 ± 0.04; 0.32 ± 0.02	7.48 ± 0.06; 0.36 ± 0.03	8.32 ± 0.04; 0.34 ± 0.02	8.09 ± 0.03; 0.37 ± 0.015
Deutero-DME Br^-	7.37 ± 0.06; 0.35 ± 0.03	7.17 ± 0.10; 0.38 ± 0.05	8.12 ± 0.05; 0.37 ± 0.025	7.78 ± 0.10; 0.38 ± 0.05

[a] For all but the chloro and azido compounds, the EPR signal was too small for good ENDOR at fields higher than 10 G above the $g_e^{\parallel}$ extremum. The chloro- and azidohemins, which have broader peak widths, enable one to follow ENDOR to higher fields. For the azides we could follow the ^{14}N ENDOR out to 30 G above the $g_e^{\parallel}$ extremum, and the ^{14}N hyperfine coupling decreased by about 0.06 MHz from its value at 10 G above the $g_e^{\parallel}$ extremum. For the chloride compound we could follow the ^{14}N ENDOR out to 15 G above the $g_e^{\parallel}$ extremum, and the nitrogen hyperfine coupling decreased by about 0.03 MHz from its value at 10 G above the $g_e^{\parallel}$ extremum. Nitrogen quadrupolar couplings for both azido and chloro compounds were found to increase by about 0.01 MHz on going out to the respective higher fields.

perfine and quadrupole couplings. If axial ligand and solvent are kept the same, the nitrogen hyperfine and quadrupole couplings show little difference between proto- and deuterohemins.

The most marked variation in nitrogen hyperfine parameters is the variation due to solvent. Figure 1 shows the approximate 0.6-MHz upward shift in nitrogen hyperfine coupling constant, $\lvert A_{zz}\rvert$, for the protohemin bromide in going from solvent I to solvent II. (A comparable shift to that seen from proto- and deuterohemins was also seen for the nitrogens of TPPFeCl and OEPFeCl upon going from THF-$CHCl_3$ to a $CHCl_3$-CH_2Cl_2 solvent, which unlike solvent II lacked diamagnetic mesoporphyrin.)

Axial Halide Hyperfine Structure. Halide hyperfine splittings seen directly by EPR for the fluoro- and bromohemins are shown in Table II. In ref 2a we reported ^{35}Cl and ^{37}Cl hyperfine couplings as determined by ENDOR with ^{35}Cl and ^{37}Cl in 3:1 natural abundance. In our present work we made protohemin chloride with ^{37}Cl in 90% enrichment. This enabled us to verify both ^{35}Cl and ^{37}Cl assignments originally made in ref 2a (Table II of ref 2a) and to calculate chloride magnetic hyperfine and quadrupole parameters here with greater precision and confidence.

As shown in Table II, the values of the axial ligand hyperfine couplings are consistently lower in solvent II than in solvent I. Figure 2 shows the difference in hyperfine splittings for the bromide nucleus (about 6%) between the two solvents. In some solvents, such as *N,N*-dimethylformamide and Me_2SO, bromide anion is quite labile, but Figure 2 shows that in solvents I and II the bromide ion is definitely bound to the heme.

We have looked for axial hyperfine structure from the other hemins. The azidohemin gives several broad ENDOR resonances in the 5–10-MHz region, which are well outside the region where proton ENDOR is found and which are in the general region where axial ligand (histidine) nitrogen hyperfine structure has been found.[2b] The only magnetic nuclei on the acetate and formate ligands are protons which are several bonds removed from the point of ligation to the iron. Since there are many other protons at a roughly equivalent distance, we have not positively identified ENDOR from the formate or acetate ligands themselves.

Proton ENDOR. Proton ENDOR was initially done to assign proton resonances to various hemin protons and to determine if solvent protons, as from THF, were giving hyperfine interactions. As discussed in eq 4, a proton which is weakly coupled to a paramagnetic electron will give two ENDOR lines, which are centered at the bulk proton NMR frequency and split apart from each other by the magnitude of the electron–proton magnetic hyperfine coupling, $\lvert A_{zz}\rvert$. As shown in Figures 3a, b, and c, respectively, we compared proton ENDOR spectra from protohemin chloride, deuterohemin chloride, and TPPFeCl, all of which were dissolved in fully deuterated solvent I (i.e., THF-d_8 and $CDCl_3$). The most striking feature is the pair of sharp proton peaks from the proto- and deuterohemins with a separation, $\lvert A_{zz}\rvert$, of about 0.8 MHz. These peaks were absent from the proton ENDOR spectrum of TPPFeCl, which lacks protons on its bridging meso carbons. Thus, we assigned the starred peaks from the proto- and deuterohemins to the meso protons.[17] As discussed below, a calculation of the expected magnetic hyperfine couplings for meso protons, based on a knowledge of hemin coordinates[18] and proton NMR contact shifts,[19] gave good agreement with the separation of the ENDOR peaks assigned to meso protons. Small differences between some of the less intense proton peaks of the three compounds were seen, and we believe that these peaks reflect the differing outer pyrrole constituents and the tetraphenylporphyrin phenyl groups.

Next we went to solvent I made with deuterated $CDCl_3$ but with protonated THF, and several new proton lines appeared with $\lvert A_{zz}\rvert$ values of 1.1 and 1.9 MHz, as shown for protohemin

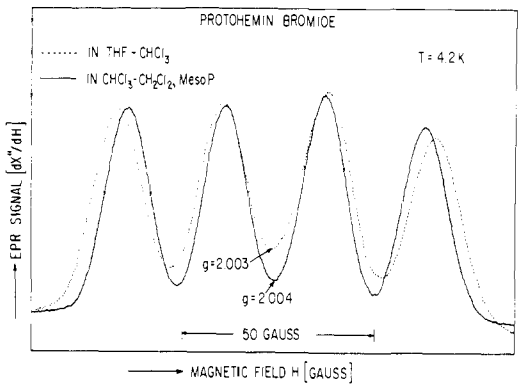

Figure 2. EPR spectrum from the bromide ligand in solvent I and solvent II. The purpose of this figure is to show a decrease in bromide hyperfine coupling brought on by going from solvent I to solvent II. $T = 4.2$ K, microwave power $\simeq 10\ \mu$W, 100-kHz field modulation $\simeq 6$ G peak to peak, and both spectra taken with 250-G field sweep in 1.0 min with a time constant of 0.01 s. In solvent I $\nu_e = 9.204$ GHz, and $g_e^{\parallel} = 2.003$ when $H = 3.283$ kG. In solvent II $\nu_e = 9.192$ GHz, and $g_e = 2.004$ when $H = 3.278$ kG.

Table II

Hyperfine couplings in MHz from axial F^-, Cl^-, and Br^- ligands

Compound	In THF-$CHCl_3$	In $CHCl_3$-CH_2Cl_2 + mesoporphyrin
Proto-DME F^-	$\lvert A_{zz}\rvert = 132.4 \pm 0.3^b$	$\lvert A_{zz}\rvert = 128.6 \pm 0.6^b$
Proto-DME $^{35}Cl^-$	$\lvert A_{zz}\rvert = 16.04 \pm 0.07$	$\lvert A_{zz}\rvert = 14.78 \pm 0.07$
	$\lvert P_{zz}\rvert = 4.07 \pm 0.02^a$	$\lvert P_{zz}\rvert = 4.33 \pm 0.02^a$
Proto-DME $^{37}Cl^-$	$\lvert A_{zz}\rvert = 13.34 \pm 0.05$	$\lvert A_{zz}\rvert = 12.28 \pm 0.2$
	$\lvert P_{zz}\rvert = 3.20 \pm 0.02^a$	$\lvert P_{zz}\rvert = 3.45 \pm 0.06^a$
Proto-DME Br^-	$\lvert A_{zz}\rvert = 76.7 \pm 0.6^b$	$\lvert A_{zz}\rvert = 72.4 \pm 0.7^b$
Deutero-DME F^-	$\lvert A_{zz}\rvert = 133.0 \pm 0.4^b$	$\lvert A_{zz}\rvert = 130.7 \pm 0.8^b$
Deutero-DME $^{35}Cl^-$	$\lvert A_{zz}\rvert = 16.16 \pm 0.12$	$\lvert A_{zz}\rvert = 15.02 \pm 0.3^a$
	$\lvert P_{zz}\rvert = 3.97 \pm 0.04^a$	$\lvert P_{zz}\rvert = 4.25 \pm 0.09^a$
Deutero-DME Br^-	$\lvert A_{zz}\rvert = 78.3 \pm 2.0^b$	$\lvert A_{zz}\rvert = 71.0 \pm 2.5^b$

^{35}Cl and ^{37}Cl ENDOR frequencies in MHz from protohemin DME[a]

In THF-$CHCl_3$		In $CHCl_3$-CH_2Cl_2 + mesoporphyrin	
$^{35}Cl^-$	$^{37}Cl^-$	$^{35}Cl^-$	$^{37}Cl^-$
1.6 (sh)			
6.90 ± 0.06	5.69 ± 0.05	6.27 ± 0.03	~5.1 est. (hidden by ^{14}N)
9.14 ± 0.03	7.65 ± 0.02	8.51 ± 0.07	7.14 ± 0.06
14.81 ± 0.04	11.89 ± 0.02	14.71 ± 0.02	11.81 ± 0.05
17.51 ± 0.04	14.25 ± 0.03	17.38 ± 0.04	14.28 ± 0.05

[a] Chloride ENDOR was performed under saturating EPR conditions at 2.1 K. These numbers were obtained while sitting at 5 G above the $d\chi''/dH$ maximum near $g_e^{\parallel} = 2.00$. ^{35}Cl ENDOR from ^{35}Cl in 75% natural abundance; ^{37}Cl ENDOR from ^{37}Cl in 90% enrichment. [b] Fluoride and bromide hyperfine structures were obtained by EPR near $g_e = 2.00$ under nonsaturating EPR conditions at 4.2 K.

chloride and TPPFeCl in Figures 3d and e, respectively. The latter two proton spectra indicate that hemins can specifically interact with THF. The THF proton resonances occurred in solvent I both from hemins with large, bulky axial anions like acetate or azide and with smaller anions like fluoride or chloride. When we used deuterated THF but protonated $CHCl_3$, we detected no new ENDOR peaks from proto- or deuterohemins, but TPPFeCl showed one set of broad proton ENDOR transitions with $\lvert A_{zz}\rvert \simeq 1.0$ MHz, which must have originated from $CHCl_3$ protons.

Figure 3f shows protons from protohemin chloride in solvent II that was made with $CDCl_3$ and CD_2Cl_2, and we note the similarity of this spectrum to that in Figure 3a. The main difference between Figures 3a and 3f is that the splitting of the

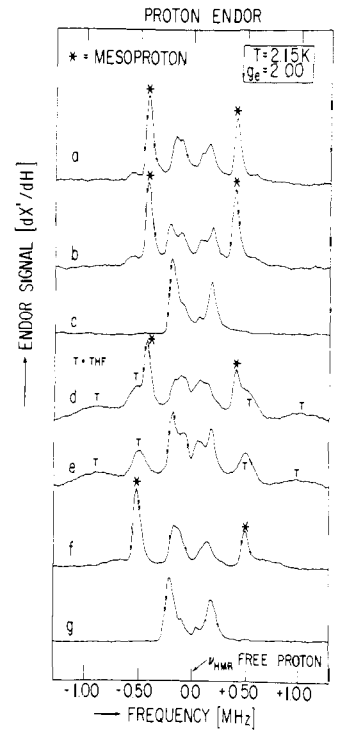

Figure 3. Proton ENDOR from hemin chloride compounds. Starred peaks are assigned to meso protons, and peaks with "T" are assigned to THF protons: (a) proton ENDOR from protohemin chloride dimethyl ester in fully deuterated THF-d_8-$CDCl_3$; (b) proton ENDOR from deuterohemin chloride dimethyl ester in fully deuterated THF-d_8-$CDCl_3$; (c) proton ENDOR from TPPFeCl in fully deuterated THF-d_8-$CDCl_3$; (d) proton ENDOR from protohemin chloride dimethyl ester in solvent I made with THF (containing H not D) and with $CDCl_3$; (e) proton ENDOR from TPPFeCl in solvent I made with THF (containing H not D) and with $CDCl_3$; (f) proton ENDOR from protohemin chloride dimethyl ester in solvent II made with $CDCl_3$ and CD_2Cl_2; (g) proton ENDOR from TPPFeCl in 1:1 (v/v) $CDCl_3$-CD_2Cl_2. Different samples cause the microwave cavity frequency to vary slightly between samples, and thus the free proton frequency will vary slightly from one sample to the next. Rather than draw separate frequency axes, we have referred each spectrum to the respective free proton frequency. Spectra were taken sitting 5 G to the high-field side of the $g_e^{\parallel} = 2.00$ extremum, $T = 2.1$ K, microwave power $\simeq 10\ \mu$W, 100-kHz field modulation $\simeq 0.15$ G peak to peak, ENDOR rf $\simeq 1.0$ G, and EPR was done in the dispersion mode.

intense peaks which we have assigned to meso protons has increased from 0.8 to 1.0 MHz. As shown in Figure 3g, the spectrum from TPPFeCl in $CDCl_3$-CD_2Cl_2 is essentially unchanged from that in THF-d_8-$CDCl_3$.

We next attempted to find changes in the meso proton ENDOR consistent with the systematic changes observed by NMR chemical shifts of meso protons,[4] and we found such changes with our hemins in solvent II. In Figure 4 we compare the proton spectrum from protohemin chloride with that from protohemin fluoride, and the separation of the meso proton peaks from the fluoride is about 0.065 MHz less than the separation of the same peaks from the chloride. The proton dipolar interaction (eq 5) is an anisotropic function of the relative orientation of hemin normal and magnetic field, and we wanted to take account of any small effect upon the measured proton hyperfine couplings of the field position where we did ENDOR. In each of our samples we measured the meso proton splittings at the $g_e^{\parallel}$ extremum and out to at least 10 G above it. Even though there may be some small variation of magnetic hyperfine coupling with field, there is still a definite trend in measured couplings with axial anion, and the trend shown in Figure 5 is consistent with previous NMR measurements.

Having found this variation of meso proton couplings in

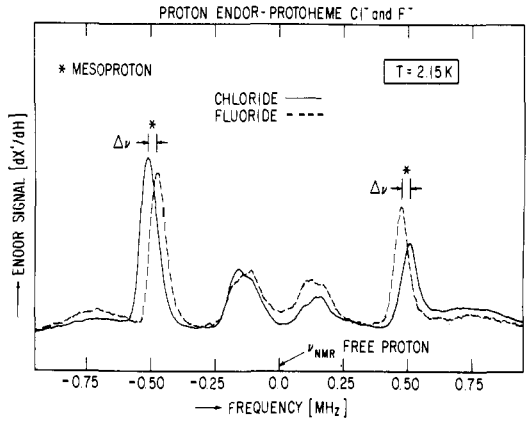

Figure 4. Proton ENDOR from protohemin chloride dimethyl ester compared with proton ENDOR from protohemin fluoride dimethyl ester. The purpose of this figure is to show the difference in meso proton separations between the two compounds. This difference is 0.065 MHz $\simeq 2\Delta\nu$. Both samples were in solvent II prepared with $CDCl_3$ and CD_2Cl_2. For ease of comparison the two spectra are referred to their respective free proton frequencies. For both samples a 100-kHz field modulation $\simeq$ 0.4 G peak to peak was used, EPR was done in the dispersion mode, and the ENDOR rf was $\simeq$ 1 G peak to peak. The ENDOR spectrum from the protohemin chloride was taken at a microwave power of $\simeq 2\ \mu$W at the $g_e^{\parallel} = 2.00$ peak extremum, and the magnetic field was 3.278 kG, corresponding to a free proton frequency of 13.96 MHz. The spectrum from the fluoride compound was taken at the peak of the high-field fluoride hyperfine pattern with a microwave power $\simeq 60\ \mu$W and at a magnetic field of 3.289 kG corresponding to a free proton frequency of 14.00 MHz.

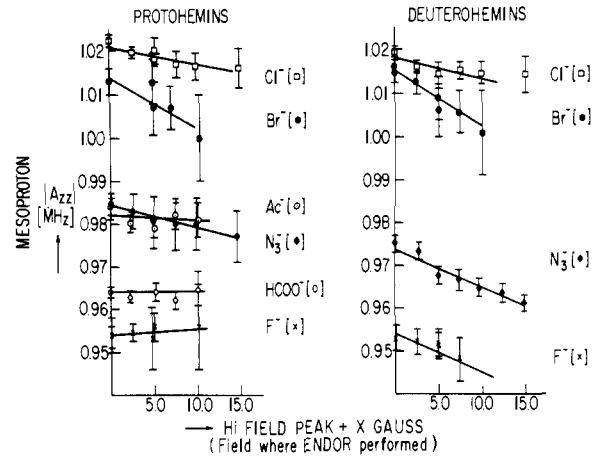

Figure 5. Hyperfine coupling $|A_{zz}|$ for the meso protons of the various anionically liganded hemin compounds, Measurements were performed in solvent II. As discussed in the text, ENDOR measurements were performed at the high-field peak extremum near $g_e^{\parallel}$ and at fields above (i.e., at X G above) this extremum in order to take into account variation of measured ENDOR frequencies with exact position on the EPR line. To obtain the necessary precision for these experiments, the ENDOR frequencies were swept slowly (~0.06 MHz/s) by the linear ramp from the signal averager over a 0.3-MHz range centered on each meso proton ENDOR line. Each point on the figure is the result of measurements of ENDOR frequencies obtained from alternately increasing and decreasing ENDOR frequency sweeps. The end points of the ENDOR frequency sweeps were stable to better than 0.001 MHz, and the klystron frequency and magnetic field were stable to at least 1 part in 10^4.

solvent II, we measured the variation of the meso proton couplings in solvent I. As indicated in Table III, the range of variation of meso proton couplings in solvent I is only about 2.5%, as opposed to 6% in solvent II. With the notable exception of fluorohemin the order of variation with ligand in solvent I appears to be the same as in solvent II.

Theory and Discussion

In the systems studied here the magnetic field points along the porphyrin normal. We interpret our data by a simple, first-order, axial spin Hamiltonian as previously used with hemin systems.[2] For a nucleus with spin I and an electron with effective spin $\frac{1}{2}$, this spin Hamiltonian (electronic Zeeman + nuclear terms) is:

$$\mathcal{H}_e = g_e^{\parallel}\beta_e H_z S_z + A_{zz} I_z S_z + P_{zz}(I_z^2 - \tfrac{1}{3}I(I+1)) - g_n\beta_n H_z I_z \quad (1)$$

where I_z and S_z are the z components of the nuclear and electronic spin operators. The first term is the electronic Zeeman interaction, A_{zz} is the z component of the magnetic hyperfine interaction, P_{zz} is the z component of the nuclear quadrupole interaction,[20] and the last term is the direct nuclear Zeeman interaction. By diagonalizing the above spin Hamiltonian, one obtains for the nucleus in question the expression ν_{ENDOR} for the ENDOR transition frequencies.

Nitrogen ENDOR. For the $I = 1$ nucleus of ^{14}N one obtains the following four ENDOR frequencies:

$$h\nu_{ENDOR} = |\tfrac{1}{2}|A_{zz}| \pm |P_{zz}| \pm g_n\beta_n H_z| \quad (2)$$

^{14}N ENDOR lines occur in two pairs, the lines in each pair being separated by twice the nuclear Zeeman energy, $g_n\beta_n H_z$. The predicted ^{14}N Zeeman splittings agree with those which we experimentally have found.[2a]

In previous single-crystal EPR work on hemin in perylene[21] the major contribution to $|A_{zz}|$ for the nitrogens was the Fermi interaction with nitrogen s orbitals.[22,23] Our work here has shown that $|A_{zz}|$ is quite insensitive to variation of axial anion,

Table III. Meso Proton Hyperfine Couplings

Compound	$\|A_{zz}\|$, MHz: In $CHCl_3$-CH_2Cl_2 + mesoporphyrin[a]	$\|A_{zz}\|$, MHz: In THF-$CHCl_3$[a]
Proto-DME F^-	0.953 ± 0.007	0.835 ± 0.004[b]
Proto-DME $HCOO^-$	0.965 ± 0.002	0.816 ± 0.003[b]
Proto-DME AC^-	0.979 ± 0.002	0.823 ± 0.003[b]
Proto-DME N_3^-	0.981 ± 0.006	0.823 ± 0.004
Proto-DME Cl^-	1.020 ± 0.003	0.831 ± 0.003[b]
Proto-DME Br^-	1.010 ± 0.007	0.827 ± 0.004[b]
Deutero-DME F^-	0.951 ± 0.003	0.840 ± 0.01
Deutero-DME N_3^-	0.968 ± 0.004	0.813 ± 0.003
Deutero-DME Cl^-	1.014 ± 0.003	0.826 ± 0.003
Deutero-DME Br^-	1.009 ± 0.005	

[a] Measured at 5 G above the peak of the $g_e^{\parallel} = 2.00$ extremum, or in the case of F^- and Br^- compounds, 5 G above the highest field peak. [b] Measured in fully deuterated THF-d_8-$CDCl_3$ to avoid any possible interference from THF protons.

and this may be because the σ-bonded hemin core, to which the nitrogen s orbitals contribute, is insensitive to the change of the axial anions that we have used. Recent theoretical predictions of Das et al.[24] indicate little change in nitrogen $|A_{zz}|$ with axial halide; they predict that $|A_{zz}|$ for chlorohemin should be about 3.5% higher than for fluorohemin and about 3.8% higher than for bromohemin.

The largest change in nitrogen hyperfine couplings that we have seen is brought on by going from solvent I to solvent II. We do not yet have a detailed explanation for this effect, but we note several relevant points. Values for the nitrogen $|A_{zz}|$ in solvent I are similar to those seen from hemin in acid metmyoglobin and methemoglobin,[2b,c] for which the hemin has $|A_{zz}|$ in the 7.5–7.6-MHz range and in which the iron

appears to be strongly bound to the proximal histidine with a sixth, presumably weakly bound, ligand derived from water. In solvent II our couplings are similar to those of hemin systems which are 5-coordinate, like hemin in perylene[21] or TPPFeCl in $CHCl_3$–CH_2Cl_2, or to systems which lack the proximal histidine, like hemoglobin $M_{Hyde\ Park}$.[2c] THF is known to be an organic base (i.e., electron donor),[25] it has been implicated as a ligand for iron(II) porphyrin,[26] and it is capable of coordinating via the oxygen to metal ions.[27] We have noted the proton peaks from THF protons of solvent I, and these peaks certainly imply a definite proximity of THF and hemin. Given the >1000-fold molar excess of THF to hemin in our systems, we suggest that THF may serve as a sixth ligand.[28] Because of the weak interaction expected between an ether oxygen and a metal ion, the binding of THF is expected to be weak; for stereochemical reasons as well, we would expect the iron(III) out of plane toward the axial anion.

Apart from acting as a ligand, THF could also perturb the hemin by interacting with the porphyrin π system[5b] or with the axial anion. The present ENDOR data are insufficient to evaluate these latter perturbations in detail. (Since the same THF pattern of proton ENDOR appears from hemins with both bulky and small anions, the implication is that the THF seen by ENDOR must be interacting with the hemin directly rather than through the axial anion.) It should be noted that the low temperatures needed for ENDOR may well alter the relative importance of solvent interactions with the metal ion, the anion, or the porphyrin π system.[28] Nevertheless, it is attractive to consider solvent I as a model for hemoproteins because of the ability of THF to serve, albeit weakly, as a sixth ligand. The differences in measured hyperfine parameters between solvent I and solvent II may then be due to the differences between hemin with 5-coordination in solvent II and hemin with 6-coordination in solvent I.

Interactions with Chloride and Other Halides. For the $I = 3/2$ ^{35}Cl or ^{37}Cl nuclei eq 1 predicts six ENDOR frequencies whose transition energies are:

$$|1/2|A_{zz}| \pm g_n\beta_n H_z| \tag{3a}$$

$$h\nu_{ENDOR} = |1/2|A_{zz}| + 2|P_{zz}| \pm g_n\beta_n H_z| \tag{3b}$$

$$|1/2|A_{zz}| - 2|P_{zz}| \pm g_n\beta_n H_z| \tag{3c}$$

In ref 2a we showed the chloride ENDOR spectrum from protohemin chloride dimethyl ester in solvent I. The four most prominent chloride peaks were assigned to ^{35}Cl, and when fit to eq 3a and 3b gave values of $|A_{zz}| = 16.1 \pm 0.1$ MHz and $|P_{zz}| = 4.0 \pm 0.1$ MHz. A low-energy ENDOR transition from eq 3c was predicted and seen in the 1.5-MHz region. Three less prominent peaks were assigned to ^{37}Cl whose natural abundance is 1/3 that of ^{35}Cl. More recent work here with 90% ^{37}Cl-enriched material has confirmed our assignment of the three weaker peaks at 5.69, 7.65, and 11.89 MHz from ^{37}Cl in solvent I and has brought out an expected fourth ^{37}Cl peak at 14.25 MHz. In ref 2a we had to use a detailed argument to obtain $|A_{zz}|$ and $|P_{zz}|$. However, now with good information from both ^{35}Cl and ^{37}Cl and with the known quadrupole and magnetic moments of ^{35}Cl and ^{37}Cl,[29] we do not need to resolve all six transitions for a particular isotope to obtain good estimates for $|A_{zz}|$ and $|P_{zz}|$.

As the halide ligand becomes less electronegative upon going from F^- to Cl^- to Br^-, the degree of covalent bonding with the iron should increase.[30] We have measured only one component of the hyperfine interaction, which may vary from one hemin halide to the next in its proportion of contact and dipolar contributions. Nevertheless, a rough measure of covalency changes from one halide to the next can be found by comparing ratios of $|A_{zz}|/g_n$ (thereby removing the nuclear magnetic moment dependence from the hyperfine coupling). The values of $|A_{zz}|/g_n$ are in the expected order: $F^- < Cl^- < Br^-$.

It has been shown theoretically[31] and empirically[32] that an inverse relation exists between the ionic character of chloride and the magnitude of the chloride quadrupole interaction. The relatively small ^{35}Cl quadrupole coupling indicates that the chloride–iron bond is fairly ionic (as opposed to covalent) though certainly not as ionic as the metal-chloride bond in LiCl.[32]

Finally, we note on changing from solvent I to solvent II the decrease in magnetic hyperfine couplings for F^-, Cl^-, and Br^- and the simultaneous increase in the quadrupole coupling of Cl^-.

Proton Hyperfine Interactions. For the $I = 1/2$ ^1H nucleus ($P_{zz} = 0$) eq 1 predicts two ENDOR transitions with frequencies:

$$h\nu_{ENDOR} = |g_n\beta_n H_z \pm 1/2|A_{zz}|| \tag{4}$$

For any given proton there will thus be two ENDOR peaks[33] centered at $g_n\beta_n H_z$ (i.e., at the free proton NMR freqeuency) and split apart from each other by the magnitude $|A_{zz}|$ of the hyperfine coupling. A_{zz} is the sum of a dipolar contribution and contact contribution.

A simple approximation for the dipolar contribution is to consider that it is between a proton and the electron spin which is localized on the heme iron.[34] The expression for the dipolar interaction is:

$$A_{dipole} = g_e||\beta_e g_n\beta_n(3\cos^2\alpha - 1)/r^3 \tag{5}$$

r is the iron-to-proton distance, and α is the angle between the vector joining the iron–proton coordinates and the external magnetic field. α is close to 90° for porphyrin protons when the magnetic field is along the normal. We have calculated proton dipolar interactions from appropriate crystallographic information for hemin[18a] and TPPFeCl.[18b]

At a distance of about 4.5 Å from the iron, the meso proton of proto- or deuterohemin is the closest porphyrin proton to the iron, and the calculated dipolar interaction for it is about −0.80 MHz. The pyrrole methyl and α-CH_2 protons have a dipolar interaction of about −0.30 MHz. For TPPFeCl the nearest protons to the iron are those on the pyrrole rings, and these have a dipolar interaction of about −0.50 MHz. Next are the ortho protons of the phenyl groups, which have a dipolar interaction of about −0.35 MHz.

Contact interactions arise from unpaired electron in proton s orbitals, and contact shifts have been estimated from NMR data.[19] For meso protons the NMR contact shifts are somewhat dependent on the solvent used. The meso proton contact shift of deuterohemin, when measured in dimethyl sulfoxide (Me_2SO) [which is a weakly coordinating solvent that can replace certain axial anions of hemins[35]], is estimated to be in the 0.03–0.10-MHz range.[19a] The contact interaction from meso protons of OEPFeCl in $CDCl_3$ is estimated at −0.27 MHz.[19b] Pyrrole methyl and α-CH_2 protons have contact shifts estimated at 0.2[19a] and 0.1[19b] MHz, respectively.[36] In TPPFeCl the contact interaction for the pyrrole protons is estimated at 0.20[19b,c] MHz and for the ortho phenyl at −0.02[19b] MHz.

To estimate the expected ENDOR frequencies for various protons we compute $|A_{zz}|$ by adding the dipolar and contact contributions and taking the absolute value of the result. Thus, protons other than meso protons are expected to have the magnitude of their hyperfine interaction $|A_{zz}| < 0.4$ MHz. The hyperfine interaction will be largest for meso protons and, depending on solvent, it is expected in the 0.71–1.1-MHz range, in agreement with separations observed for our assigned meso proton ENDOR lines. The major contribution to $|A_{zz}|$ for meso protons is the dipolar contribution. In ENDOR measurements, as opposed to solution NMR, the dipolar interaction is not averaged out.

In solvent II we noted variation of meso proton ENDOR frequencies in agreement with variation of NMR chemical shifts of the same protons.[4] We discuss some details of that agreement here. The NMR chemical shifts (reported at 35 °C in $CDCl_3$ and measured relative to Me_4Si) for the meso protons of fluoro-, azido-, chloro-, and bromodeuterohemin dimethyl esters increase in the order 35, 46, 57, and 57 ppm.[4] Errors in these chemical shifts were not given, but the meso proton NMR peaks vere quite broad, and we estimate the errors at several parts per million. To determine if non contact terms may be contributing to the NMR shifts, it is appropriate to measure shifts over a range of temperatures, as has been done by La Mar et al.[19b,c] for several TPPFe and OEPFe compounds. In particular the pseudocontact interaction may be important for protons.[19b,c] The pseudocontact interaction arises in solution NMR when electronic anisotropy prevents the electron–proton dipolar interaction from being completely averaged out. However, as discussed in footnote 37, the pseudocontact interaction is insufficient in magnitude and of incorrect sign to account for the variation seen in the meso proton chemical shifts in deuterohemins.[4]

The expression for the NMR contact shift of high-spin ferric compounds is given in terms of A_{con} (the Fermi contact interaction in hertz) as:[38]

$$(\Delta\nu/\nu)_{con} = (A_{con}/h)(35g_e\beta_e/12k(\gamma_H/2\pi))/T \qquad (6)$$

where k is Boltzmann's constant, γ_H = proton magnetogyric ratio, and T is the absolute temperature. A contact shift change of 22 ppm at 35 °C, such as seen between fluoride and chloride compounds, translates into a change in contact interaction of −0.07 MHz. Such a negative change, when combined with the much larger negative dipolar interaction for the meso protons, predicts an increase of 0.07 MHz in the value of $|A_{zz}|$. This predicted increase is in good agreement with the 0.065-MHz increase seen by ENDOR.

The variation in ENDOR frequencies shown in Figure 5 could conceivably, if there were no available complementary NMR data, be related to a small variation in the dipolar interaction (eq 5). However, such a small variation in dipolar interaction cannot account for the variation in chemical shifts seen by NMR.[4] The consistent explanation of both NMR and ENDOR results for the meso protons is that they are both due to a change in the Fermi contact interaction. Since the dipolar interaction for a meso proton is negative and of order −0.80 MHz, then the overall contact contribution for the meso proton must also be negative and of order −0.20 MHz to obtain $|A_{zz}| \simeq 1.00$ MHz. The contact contribution for the meso proton will be negative if it arises by exchange polarization of spin from the adjacent carbon π orbital.[39] According to ref 19b, the unpaired electron spin will have been transferred from the iron to the meso carbon by interaction between the metal d_π and the lowest vacant $e(\pi)$ porphyrin orbital. In solvent II the axial anion is able to affect the strength of this interaction between metal and porphyrin.

In solvent I the measured value of $|A_{zz}|$ is only slightly larger than the dipolar value of 0.80 MHz. This implies that the meso proton contact interaction is smaller in magnitude than in solvent II, and the variation of this contact interaction with axial anion is also smaller. Apparently interaction of the hemin with THF renders the meso carbon spin density less susceptible to change in axial anion. We have previously noted the similarity in the nitrogen hyperfine couplings found in solvent I and in metmyoglobin and methemoglobin. In acid metmyoglobin and metmyoglobin fluoride, we find mesoproton $|A_{zz}|$ values of 0.79 and 0.82 MHz, respectively; these $|A_{zz}|$ values are very similar to those for the hemin meso protons in solvent I.

We show in Figures 3d and 3e the THF proton ENDOR. We do not know the proportion of contact and dipolar interaction for these protons. However, we can show that the measured hyperfine couplings of 1.1 and 1.9 MHz are consistent with dipolar interactions from the THF protons, where the THF oxygen is 2 to 3 Å from the hemin iron and along the hemin normal.

Future Work

We have largely confined the work in this paper to proto- and deuterohemins. We have done this because these compounds are similar to hemin as it naturally occurs in proteins, and because much of the previous work by other techniques has been done on these compounds.[3–5] Because of the tendency of these hemins to aggregate in solution we have had to devise fairly elaborate solvent systems (i.e., solvents I and II). Work presently in progress on TPPFe and OEPFe compounds dissolved in a 1:1 $CHCl_3$–CH_2Cl_2 glass (no mesoporphyrin present) shows that we do not need so elaborate a solvent system to prevent their aggregation. We are also extending ENDOR measurements to hemoproteins having various axial anions.

Acknowledgments. We are grateful to Professor Y. P. Myer of the Department of Chemistry, SUNY/Albany, in whose lab many of the chemical preparations were carried out, and to M. L. Smith for infrared spectra. We had several stimulating discussions with Drs. T. P. Das and J. Chang of the Physics Department, SUNY/Albany, who are simultaneously performing theoretical calculations on the same compounds upon which we do ENDOR. This work was supported by NIH Grant No. AM 17884 (C.P.S.), National Institutes of Health Biomedical Institutional Grant No. 5 S07 RR 07122-08 (C.P.S.), and Grant No. HL-15980 (W.S.C.). C.P.S. is the recipient of National Institutes of Health Research Career Development Award No. 1 K04 AM00274-01.

References and Notes

(1) (a) State University of New York at Albany; (b) Colorado State University.
(2) (a) H. L. Van Camp, C. P. Scholes, and C. F. Mulks, *J. Am. Chem. Soc.*, **98**, 4094–4098 (1976); (b) C. P. Scholes, R. A. Isaacson, and G. Feher, *Biochim. Biophys. Acta*, **263**, 448–452 (1972); (c) G. Feher, R. A. Isaacson, C. P. Scholes, and R. L. Nagel, *Ann. N.Y. Acad. Sci.*, **222**, 86–101 (1973); (d) C. P. Scholes, R. A. Isaacson, T. Yonetani, and G. Feher, *Biochim. Biophys. Acta*, **322**, 457–462 (1973); (e) C. P. Scholes and H. L. Van Camp, *Biochim. Biophys. Acta*, **434**, 290–296 (1976).
(3) (a) P. L. Richards, W. S. Caughey, H. Eberspaecher, G. Feher, and M. Malley, *J. Chem. Phys.*, **47**, 1187–1188 (1967); (b) G. C. Brackett, P. L. Richards, and W. S. Caughey, *ibid.*, **54**, 4383–4401 (1971); (c) T. H. Moss, A. J. Bearden, and W. S. Caughey, *ibid.*, **51**, 2624–2631 (1969).
(4) W. S. Caughey and L. F. Johnson, *J. Chem. Soc. D*, 1362–1363 (1969).
(5) (a) W. S. Caughey, H. Eberspaecher, W. H. Fuchsman, and S. McCoy, *Ann. N.Y. Acad. Sci.*, **153**, 722–737 (1968); (b) W. S. Caughey in "Inorganic Biochemistry", G. L. Eichhorn, Ed., Elsevier, Amsterdam, 1973, pp 797–831.
(6) Reference 5b, p 824.
(7) H. L. Van Camp, C. P. Scholes, and R. A. Isaacson, *Rev. Sci. Instrum.*, **47**, 516–517 (1976).
(8) (a) J. O. Alben, W. H. Fuchsman, C. A. Beaudreau, and W. S. Caughey, *Biochemistry*, **7**, 624–635 (1968); (b) N. Sadasivan, H. I. Eberspaecher, W. H. Fuchsman, and W. S. Caughey, *ibid.*, **8**, 534–541 (1969).
(9) In the initial studies in ref 2a on chloro- and bromohemins in THF–$CHCl_3$ we added a tenfold molar excess relative to hemin of appropriate halide ligand in the form of tetrabutyalmmonium halide. We did this as a precaution against conceivable replacement of the axial halide by THF. In our present EPR and ENDOR measurements we have determined that adding the additional halide ligand in this way was an unnecessary precaution. Because their presence would be an additional variable in a solvent system that is already complex, we decided to dispense with tetrabutylammonium salts for this work.
(10) Y. Hsu, *Mol. Phys.*, **21**, 1087–1103 (1971).
(11) J. Peisach, W. E. Blumberg, S. Ogawa, E. A. Rachmilewitz, and R. Oltzik, *J. Biol. Chem.*, **246**, 3342–3355 (1971).
(12) Fluoride hyperfine structure with a splitting of 24 G has been seen near $g_e = 6$ in crystals of metmyoglobin fluoride; M. Kotani and H. Morimoto, "Magnetic Resonance in Biological Systems", A. Ehrenberg, et al., Ed., Pergamon Press, Oxford, 1967, pp 135–140.
(13) In both solvents I and II proto- and deuterohemin azides showed another species with axial symmetry. It does not appear from ENDOR that the axial and the rhombic species of azidohemins differ in their nitrogen or proton couplings, as measured near $g_e^{\parallel} = 2.00$.

(14) The width (peak width at half-height) of the $g_e^{\parallel} = 2.00$ peak is about 14 G for the acetato- and the formatohemins and 14 G for the individual peaks of the fluoro and bromo hyperfine patterns. This 14-G width is essentially due to unresolved ^{14}N and ^{1}H hyperfine structure. Chlorohemins have a peak width of about 23 G, reflecting additional unresolved chloride hyperfine structure. All of these foregoing peaks are symmetric. The peak from the azidohemin is about 40 G wide and skewed toward higher field. In work connected with ref 2c on methemoglobins with rhombic perturbations, we have previously seen such skewed $d\chi''/dH$ line shapes near $g_e = 2.00$.
(15) (a) J. E. Bennett, J. F. Gibson, and D. J. E. Ingram, *Proc. R. Soc. London, Ser. A*, **240**, 67–82 (1957); (b) J. E. Bennett, J. F. Gibson, D. J. E. Ingram, T. M. Haughton, G. A. Kerkut, and K. A. Munday, *ibid.*, **262**, 395–408 (1961); (c) G. A. Helcké, D. J. E. Ingram, and E. F. Slade, *Proc. R. Soc. London, Ser. B*, **169**, 275–288 (1968).
(16) The $g_e^{\parallel}$ axis of the hemins upon which we are doing magnetic resonance should become slightly better oriented along the magnetic field if we can go to higher magnetic fields above the $g_e^{\parallel} = 2.00$ extremum. Of course, the EPR signal and hence the ENDOR signal very rapidly diminish in intensity above the $g_e^{\parallel} = 2.00$ extremum.
(17) In recent measurements on OEPFeCl, which also has meso protons, we observed these intense meso proton peaks at very similar separations to those seen in proto- and deuterohemin.
(18) (a) D. F. Koenig, *Acta Crystallogr.*, **18**, 663–673 (1965); (b) J. L. Hoard, G. H. Cohen, and M. D. Glick, *J. Am. Chem. Soc.*, **89**, 1992–1996 (1967).
(19) (a) R. J. Kurland, R. G. Little, D. G. Davis, and C. Ho, *Biochemistry*, **10**, 2237–2246 (1971); (b) F. A. Walker and G. N. La Mar, *Ann. N.Y. Acad. Sci.*, **206**, 328–348 (1973); (c) G. N. La Mar, G. R. Eaton, R. H. Holm, and F. A. Walker, *J. Am. Chem. Soc.*, **95**, 63–75 (1973).
(20) Quadrupole couplings are often given by the expression e^2Qq_{zz}, where eQ = nuclear quadrupole moment and $eq_{zz} = z$ component of the electric field gradient. $e^2Qq_{zz} = 4I(2I-1)P_{zz}/3$: T. P. Das and E. L. Hahn, "Nuclear Quadrupole Resonance Spectroscopy, Academic Press, New York, N.Y., 1958, Chapter 1.
(21) C. P. Scholes, *J. Chem. Phys.*, **52**, 4890–4895 (1970).
(22) In ref 21 we reported for heme nitrogens that $A_{zz} = 8.18 \pm 0.34$ MHz, of which the Fermi contribution was 8.68 ± 0.16 MHz and the dipolar contribution was -0.50 ± 0.30 MHz. The Fermi interaction can be accounted for by about 2.7% of an unpaired electron in each heme nitrogen 2s orbital.
(23) Although the intrinsic nitrogen hyperfine tensor is quite isotropic, the effective spin Hamiltonian is made highly anisotropic by the highly anisotropic g values of heme. As shown in ref 21, the magnetic hyperfine couplings increase rapidly with angle away from $g_e^{\parallel}$.
(24) M. K. Mallick, J. C. Chang, and T. P. Das, *J. Chem. Phys.*, in press.
(25) J. E. Huheey, "Inorganic Chemistry: Principles of Structure and Reactivity", Harper & Row, New York, N.Y., 1972, p 247, Table 7.4.
(26) D. Brault and M. Rougee, *Biochemistry*, **13**, 4591–4597, 4598–4602 (1974).
(27) THF acts through its oxygen as a weak ligand for molybdenum, as shown by: L. Ricard, P. Karagiannidis, and R. Weiss, *Inorg. Chem.*, **12**, 2179–2182 (1973).
(28) In room temperature solutions the visible and Soret spectra of protohemin chloride change slightly in intensity and extinction upon changing in a stepwise manner from 100% $CHCl_3$ to 100% THF. A definite color change occurs on freezing.
(29) See "Handbook of Chemistry and Physics", 55th ed, Chemical Rubber Publishing Co., Cleveland, Ohio, 1974, p E-69.
(30) J. Owen and J. H. M. Thornley, *Rep. Prog. Phys.*, **29**, 675–728 (1966). See in particular p 710.
(31) Reference 20, Chapter 7.
(32) Reference 25, p 171, Table 4.12.
(33) It is not surprising to find unequal intensities of the two ENDOR peaks from the same proton. An explanation for unequally intense ENDOR transitions from the same $I = 1/2$ nucleus is given by: E. R. Davies and T. F. Reddy, *Phys. Lett. A*, **31**, 398–399 (1970).
(34) A calculation of the dipolar contribution from unpaired electron spin distributed in molecular orbitals over the entire heme is presently being done by workers of T. P. Das.
(35) Control ENDOR experiments were done on bromohemin dissolved in 1:1 (v/v) Me_2SO–$CHCl_3$. We found that the bromide ligand was totally replaced in this solvent, and a comparison of proton ENDOR in deuterated and nondeuterated solvents showed well-defined proton ENDOR from the Me_2SO. The hyperfine interaction measured from meso protons in this solvent was $|A_{zz}| = 0.795$ MHz.
(36) Contact shifts measured by solution NMR from methyl or α-CH_2 groups will be motionally averaged quantities due to rapid rotation of such groups in solution. At liquid helium temperatures such rotation may cease, and since the contact interaction varies markedly with rotation angle for such a group, different protons on the same carbon can have different contact interactions. It is conceivable that the small peaks or shoulders seen in fully deuterated solvents which lie just outside the meso proton peaks (Figures 3a,b,f) are from such immobilized protons. For a discussion of contact interaction from such protons see: A. Carrington and A. D. McLachlan, "Introduction to Magnetic Resonance", Harper & Row, New York, N.Y., 1967, Section 7.9.
(37) An expression for the pseudocontact shift is given in eq 3, ref 19b. The pseudocontact shift depends linearly on the zero-field splitting D and inversely on T^2, where T is the absolute temperature. There is also a dipolar geometric factor similar to eq 5 in this paper. For a D of 10 cm^{-1} at T = 35 °C the pseudocontact shift for meso protons would be about −14 ppm; the negative sign comes from the negative sign of the geometric factor for meso protons. For proto- or deuterohemin fluorides D is about 5 cm^{-1}, and all the D values for the hemin compounds used here are larger than for fluoride.[3] We have calculated the change in pseudocontact interaction expected on going from deuterohemin fluoride ($D = 5.55$ cm^{-1}) to deuterohemin chloride ($D = 8.95$ cm^{-1}). This change of −5 ppm is smaller and of a different sign from the change actually seen be NMR on going from fluoro- to chlorodeuterohemin.
(38) Reference 19b, eq 2.
(39) Reference 36, Section 6.4.2.

Phosphorus-31 Nuclear Magnetic Resonance Chemical Shielding Tensors of L-*O*-Serine Phosphate and 3′-Cytidine Monophosphate

Susan J. Kohler and Melvin P. Klein*

Contribution from the Laboratory of Chemical Biodynamics, Lawrence Berkeley Laboratory, University of California, Berkeley, California 94720. *Received March 22, 1977*

Abstract: ^{31}P nuclear magnetic resonance chemical shielding tensors have been measured from single crystals of L-*O*-serine phosphate and 3′-cytidine monophosphate. The principal elements of the shielding tensors are −48, −2, and 51 ppm for serine phosphate and −68, −13, and 64 ppm for 3′-cytidine monophosphate, relative to 85% H_3PO_4. In both cases four orientations of the shielding tensor on the molecule are possible; in both instances one orientation correlates well with the P–O bond directions. This orientation of the shielding tensor places the most downfield component of the tensor in the plane containing the two longest P–O bonds and the most upfield component of the shielding tensor in the plane containing the two shortest P–O bonds. A similar orientation was reported for the ^{31}P shielding tensor of phosphorylethanolamine and a comparison is made between the three molecules.

The recently developed high-resolution multiple pulse and cross-polarization nuclear magnetic resonance (NMR) techniques have made it possible to resolve chemical shifts in solids, and therefore to accurately determine chemical shielding tensors.[1,2] Shielding tensors are intrinsically interesting in that they reflect the distribution of electronic orbitals around the nucleus. Several theoretical approaches have been used with varying degrees of success to predict shielding tensors.[3,4] On a less theoretical level, shielding tensors serve as a monitor of the chemical environment of the nucleus, and are useful in the